SCIENTIFIC ARTICLE

In Vivo Kinematics of the Scaphoid, Lunate, Capitate, and Third Metacarpal in Extreme Wrist Flexion and Extension

Michael J. Rainbow, PhD, Robin N. Kamal, MD, Evan Leventhal, PhD, Edward Akelman, MD, Douglas C. Moore, MS, Scott W. Wolfe, MD, Joseph J. Crisco, PhD

Purpose Insights into the complexity of active *in vivo* carpal motion have recently been gained using 3-dimensional imaging; however, kinematics during extremes of motion has not been elucidated. The purpose of this study was to determine motion of the carpus during extremes of wrist flexion and extension.

Methods We obtained computed tomography scans of 12 healthy wrists in neutral grip, extreme loaded flexion, and extreme loaded extension. We obtained 3-dimensional bone surfaces and 6-degree-of-freedom kinematics for the radius and carpals. The flexion and extension rotation from neutral grip to extreme flexion and extreme extension of the scaphoid and lunate was expressed as a percentage of capitate flexion and extension and then compared with previous studies of active wrist flexion and extension. We also tested the hypothesis that the capitate and third metacarpal function as a single rigid body. Finally, we used joint space metrics at the radiocarpal and midcarpal joints to describe arthrokinematics.

Results In extreme flexion, the scaphoid and lunate flexed 70% and 46% of the amount the capitate flexed, respectively. In extreme extension, the scaphoid extended 74% and the lunate extended 42% of the amount the capitates extended, respectively. The third metacarpal extended 4° farther than the capitate in extreme extension. The joint contact area decreased at the radiocarpal joint during extreme flexion. The radioscaphoid joint contact center moved onto the radial styloid and volar ridge of the radius in extreme flexion from a more proximal and ulnar location in neutral.

Conclusions The contributions of the scaphoid and lunate to capitate rotation were approximately 25% less in extreme extension compared with wrist motion through an active range of motion. More than half the motion of the carpus when the wrist was loaded in extension occurred at the midcarpal joint.

Clinical relevance These findings highlight the difference in kinematics of the carpus at the extremes of wrist motion, which occur during activities and injuries, and give insight into the possible etiologies of the scaphoid fractures, interosseous ligament injuries, and carpometacarpal bossing. *(J Hand Surg 2013;xx:. Copyright © 2013 by the American Society for Surgery of the Hand. All rights reserved.)*

Key words Carpal, kinematics, lunate, passive, scaphoid.

From the Bioengineering Laboratory, Department of Orthopaedics, Warren Alpert Medical School of Brown University and Rhode Island Hospital, Providence, RI; and the Hand and Upper Extremity Center, Hospital for Special Surgery, Weill Medical College of Cornell University, New York, NY.

The authors thank Dr. Michael J. Bey and Roger Zauel at the Henry Ford Hospital for providing the joint contact center algorithm. They also thank Daniel L. Miranda at Brown University for assistance in implementing the algorithm.

Received for publication July 1, 2011; accepted in revised form October 20, 2012.

Funded by National Institutes of Health Grants HD052127 and AR053648.

No benefits in any form have been received or will be received related directly or indirectly to the subject of this article.

Corresponding author: Joseph J. Crisco, PhD, Bioengineering Laboratory, Department of Orthopaedics, Warren Alpert Medical School of Brown University and Rhode Island Hospital, 1 Hoppin Street, CORO West, Suite 404, Providence, RI 02903; e-mail: joseph_crisco@brown.edu.

0363-5023/13/xx0x-0001$36.00/0
http://dx.doi.org/10.1016/j.jhsa.2012.10.035

THE *IN VIVO* 3-DIMENSIONAL kinematic patterns of the carpals during active wrist extension and flexion are well documented and have been shown to be consistent across people.[1–5] However, the wrist can also be loaded in extreme extension or extreme flexion,[6,7] and the corresponding kinematic patterns of the carpals have not been determined. Studying carpal kinematics at the extremes of motion may be important because the carpal ligaments are likely to be strained and injuries are more likely to occur in these positions.

Extreme loaded extension is a common wrist position in occupational settings (eg, carpentry, plumbing), sports activities (eg, pushup, yoga, Pilates, gymnastics), and activities of daily living (eg, opening heavy door, supporting body weight while leaning).[8] The wrist also achieves this posture during a fall onto an outstretched hand.[6,9,10] Whereas extreme loaded flexion is less frequently achieved than extreme extension during normal physiologic motion, certain manual occupational activities or playing string instruments require the wrist to be maintained in an acutely flexed position.

The carpals follow consistent kinematic patterns through 60° wrist flexion and 60° extension.[2,3,11–14] Averaged together, 3-dimensional studies report that the scaphoid flexes 70% and the lunate flexes 45% of the amount the capitate flexes during wrist flexion. In extension, the scaphoid and capitate extend nearly as a single rigid body, whereas the lunate extends approximately 65% the amount the capitate extends. Furthermore, it is well documented that the third metacarpal and capitate are normally tightly bound throughout this range of wrist motion.[15,16]

Arthrokinematics, as opposed to standard kinematics analysis of whole bones, pertains to the movement of bone surfaces in a joint. Measures of arthrokinematics include the joint contact area and center. Joint contact area describes the area on the subchondral bone surface that is within a threshold distance from a mating bone surface. The center of this area is weighted by the distances within the joint contact area and is mathematically similar to the center of pressure. Combining arthrokinematics with standard kinematics may provide a more thorough understanding of the carpal mechanism because these measures can thoroughly describe kinematic changes and the effects of loading at the joint surfaces.

Studying kinematic and joint space changes of the carpus during extreme passive motions should advance our understanding of common injury patterns that occur during these positions and identify deviations from active wrist kinematics. Therefore, the purpose of this study was to describe the kinematic patterns of the scaphoid, lunate, and capitate when the wrist is passively loaded at the extremes of motion. We describe these patterns using a full 3-dimensional analysis, in terms of percentage of capitate rotation and using arthrokinematics. Our expectation was that the percentage of rotation of the scaphoid and lunate to rotation of the capitate would differ between active and extreme loaded motions. In addition, we tested the following hypotheses: The capitate and third metacarpal will behave as a single rigid body at the extremes of motion, and the joint contact area and center of the radiocarpal and midcarpal joints will differ at extreme flexion and extension compared with the neutral position.

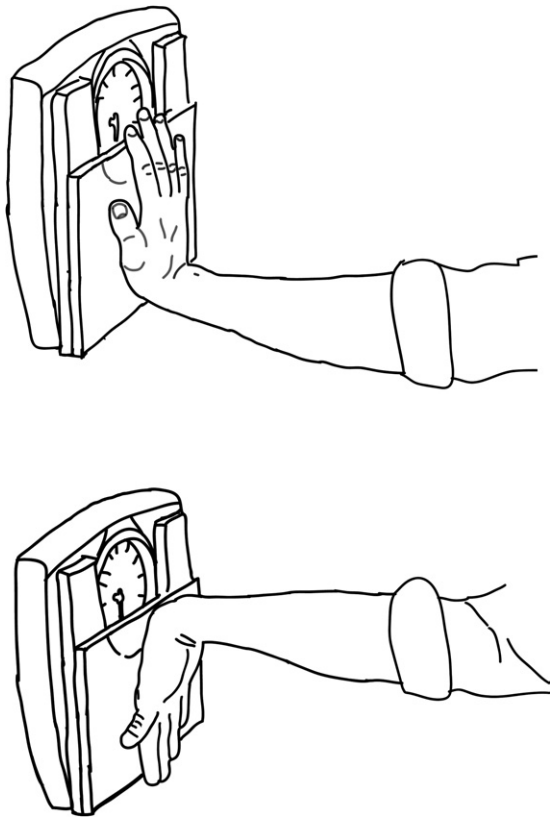

FIGURE 1: Extreme loaded extension (top) and extreme loaded flexion (bottom).

MATERIALS AND METHODS

Scanning protocol

After we obtained institutional review board approval and informed consent, a hand surgeon screened 12 right-handed volunteers (6 men and 6 women; mean age, 25 ± 4 y) with posteroanterior and lateral radiographs and physical examination to confirm the lack of injury or diseases that could affect carpal motion. We obtained computed tomography (CT) volume images of

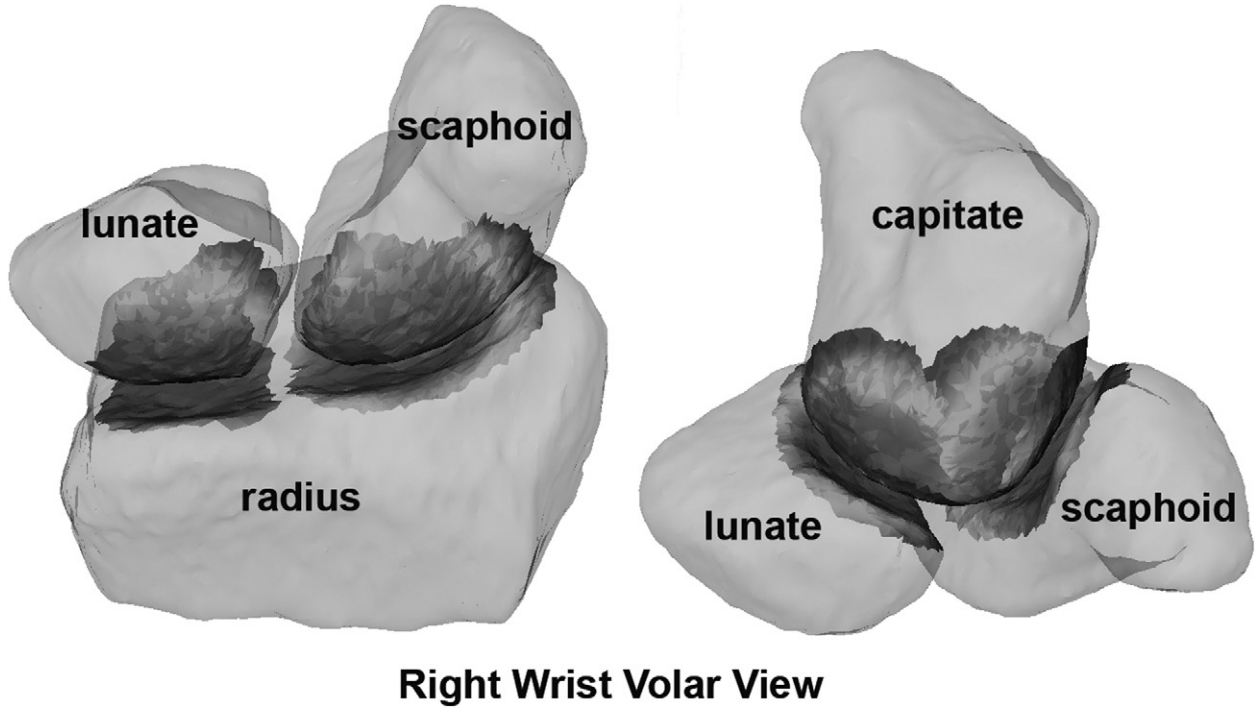

FIGURE 2: The 2.5-mm threshold for the radiocarpal joints (left) and midcarpal joints (right) of a representative subject. The 2.5-mm contour captured the entire articular surface when the wrist was in the neutral grip position.

the wrist during 3 tasks: neutral grip, extreme flexion, and extreme extension. Volunteers were positioned prone on the CT table (chests supported with a pillow) with the forearms pronated and the right arms extended, in neutral shoulder abduction, and parallel with the center axis of the CT gantry. Wrist position was not constrained.

We acquired CT volume images with a GE LightSpeed 16 CT scanner (General Electric, Milwaukee, WI) at tube settings of 80 kVp and 80 mA, a slice thickness of 0.6 mm, and a field of view that yielded an in-plane resolution of 0.3 × 0.3 mm. During the neutral grip scan, subjects held a plastic dowel (28 mm in diameter) with a relaxed grip and the forearm flat to the bed of the scanner. We required that the carpus be loaded such that it moved beyond the active range of motion. Therefore, we obtained extreme loaded extension by instructing patients to maintain an extended elbow and apply approximately 98 N by pushing with the palm of the hand against an analog weight scale that was oriented vertically and fixed to the scanner table (Fig. 1). Because there were scarce data on acceptable *in vivo* load values, we chose the load of 98 N to be consistent with the loaded condition reported in previous cadaveric studies.[17–19] Extreme loaded flexion is not a load-bearing position; therefore, in the interest of safety, subjects were not required to maintain a target load. Instead, subjects achieved extreme loaded flexion by placing the dorsal aspect of the hand flat to the scale, and extending the arm to passively flex the wrist until they felt slight discomfort in the wrist.

Image processing and kinematics

An established markerless bone segmentation and registration method[20,21] generated bone surface models and 6-degree-of-freedom kinematic transforms for the third metacarpal, capitate, scaphoid, lunate, and radius. We segmented the bone surface models from the neutral grip CT volume image using Mimics 9.11 (Materialize, Leuven, Belgium). Custom C++ (GNU gcc; Free Software Foundation, Boston, MA) and Matlab (The MathWorks, Natick, MA) code calculated the kinematic transformation of each bone independently from neutral grip to extreme flexion and to extreme extension.[21]

Kinematic variables were described with respect to a radial coordinate system (RCS).[22,23] The proximally directed X-axis defined pronation-supination. The radially directed Y-axis defined the flexion-extension axis, and the volarly directed Z-axis defined ulnar-radial deviation. The origin of the RCS was located at the intersection of the radiocarpal surface of the radius and the X-axis. We defined wrist flexion-extension and radial-ulnar deviation

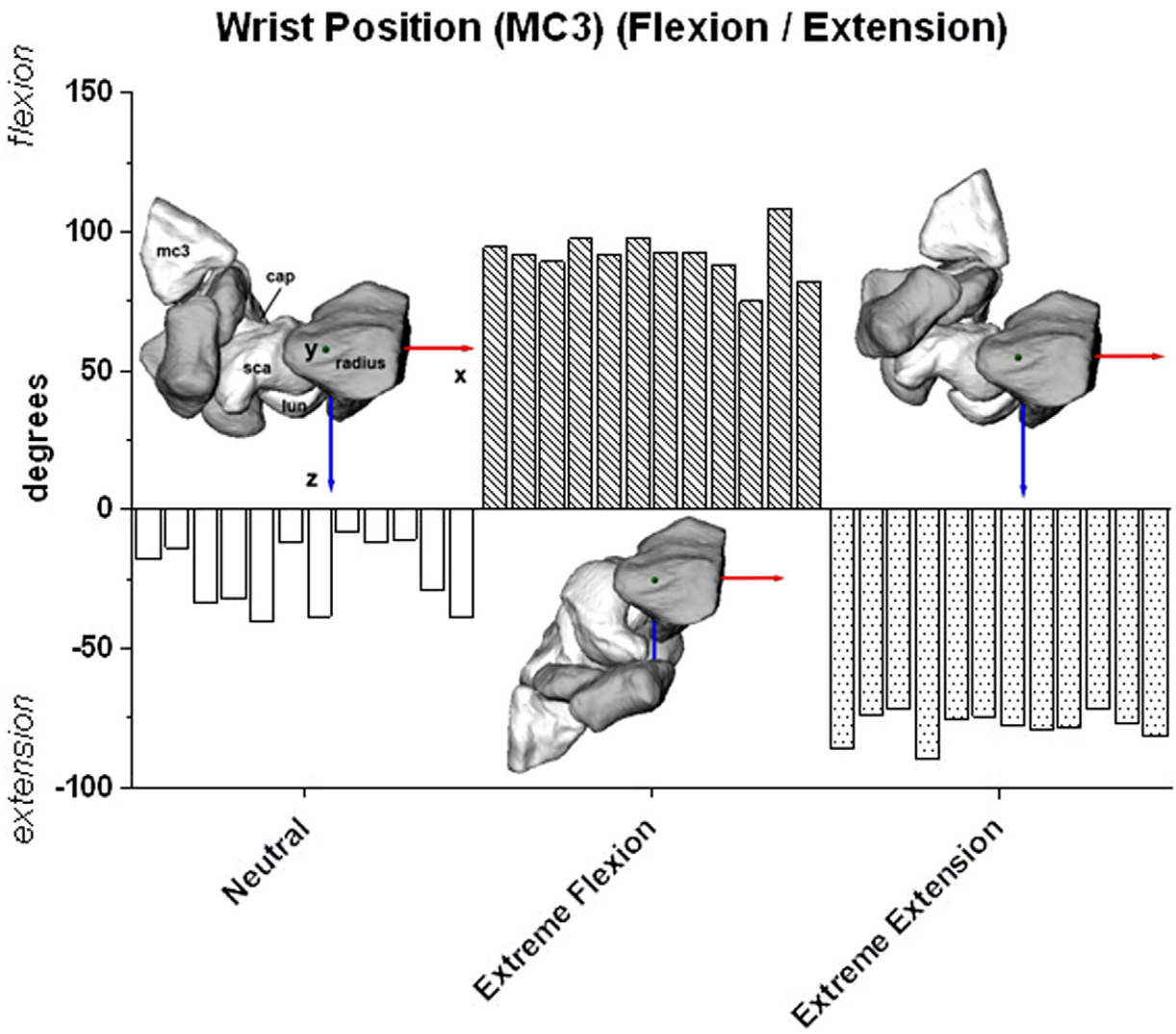

FIGURE 3: Wrist flexion and extension of all 12 subjects determined by the third metacarpal with respect to the radius. An image of a radial view of a right wrist is also included, indicating (left) neutral grip (middle) extreme flexion, and (right) extreme extension. Wrist positions were consistent across subjects, with standard deviations of 13°, 8 °, and 5 ° for neutral grip, extreme flexion, and extreme extension, respectively.

positions by the orientation of the long axis of the third metacarpal with respect to the RCS.[22]

The rotations and translations of the individual carpals from neutral grip to extreme flexion and extension were described using helical axis of motion variables. The helical axis of motion fully describes the 3-dimensional kinematics of a rigid body by defining a unique rotation axis about which the body rotates and translates. The location of the rotation axis is described here as its point of intersection with the sagittal plane (X-Z) of the RCS. The X-coordinate of this point of intersection corresponded to the proximal-distal location and the Z-coordinate corresponded to the volar-dorsal location.

Scaphoid and lunate rotation

We computed the rotation of the scaphoid and lunate as a percentage of capitate rotation. The percentage described each bone's contribution to capitate rotation. It was computed by multiplying the slope of a regression line by 100. The regression line independently fit each bone's rotation from neutral grip to extreme flexion, and neutral grip to extreme extension as a function of capitate flexion and extension.[14]

Arthrokinematics

We examined joint contact area and center between the radioscaphoid, radiolunate, scaphocapitate, and capitolunate joints. The surface mesh of each bone model consisted of vertex points and triangular connections.

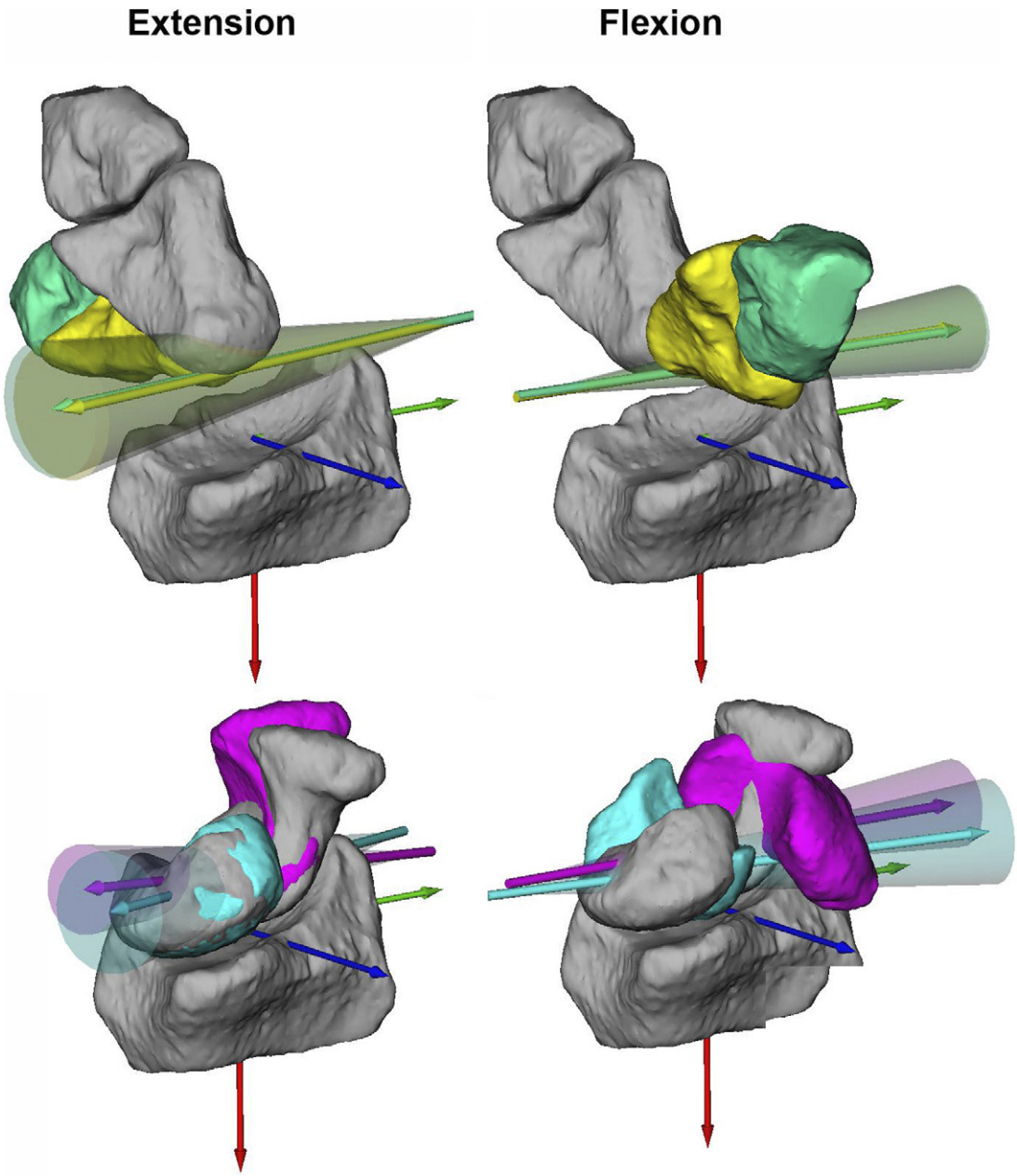

FIGURE 4: Resultant rotation axes of the third metacarpal (green) and capitate (yellow) (top) and scaphoid (purple) and lunate (turquoise) (bottom) for wrist motion from neutral grip (gray) to extreme extension and extreme flexion. We computed the resultant axes from each subject's rotation axis. The translucent cones represent variability in the angle formed by each subject's rotation axis and the resultant axis. The angular variability is calculated from vectors of unit length and is placed at the origin of the vector in the figure for illustration purposes.

We computed the joint contact area on each bone as the area of all triangles that were located within a threshold distance of 2.5 mm or less from the opposing joint surface. We selected the threshold value of 2.5 mm because it approximately captured the entire articular surface of the joints in a neutral posture in this study (Fig. 2).[24] Each triangle within the joint contact area was assigned a weight that was proportional to its area and inversely proportional to its distance from the neighboring bone. We computed the joint contact center as the central point of the weighted triangles included in the contact area. In other words, the contact center was biased toward locations on the articular surface where triangles were closer to the neighboring bone. We computed the contact area at each wrist position and reported it as the percent change from the neutral grip position. The joint contact center was visualized as a point on the bone surface, and its change

TABLE 1. Unit Vector Components Describing Orientation of the Rotation Axis for Each Bone (Third Metacarpal) From Neutral Grip to Extreme Flexion and Extreme Extension, Reported in the Radius-Based Coordinate System*

Bone	Position	X	Y	Z	Variation With Rotation Axis (°)
Third metacarpal	Extension	0.001	–0.996	0.084	8.8
	Flexion	0.038	0.999	−0.025	5.5
Capitate	Extension	−0.003	−0.993	0.115	8.8
	Flexion	0.032	0.999	−0.029	5.3
Scaphoid	Extension	−0.131	−0.957	0.259	5.7
	Flexion	0.012	0.999	−0.019	5.6
Lunate	Extension	−0.070	−0.924	0.376	7.8
	Flexion	0.002	0.986	0.168	6.6

*X, Y, and Z are the components of pronation-supination, flexion-extension, and ulnar-radial deviation, respectively. Variation with rotation axis was the mean angle between each subject's rotation axis and the resultant rotation axis of all subjects.

in location was quantified as the distance from its location in neutral grip. Each joint examined has a pair of contact centers associated with each position, and we differentiated them, for example, as follows: The radius-scaphoid contact center was located on the surface of the radius, whereas the scaphoid-radius contact refers to the contact center located on the surface of the scaphoid.

Statistical analysis

The position of the wrist in neutral grip, extreme flexion, and extreme extension across all subjects was reported as the average ± 1 standard deviation. The orientation of the rotation axes of the carpals was reported as vector components in the RCS. We defined between-subject variability of the rotation axis as the average angle between each subject's rotation axis and the resultant rotation axis of all subjects. A 2-way repeated measures analysis of variance followed by a Holm-Sidak pairwise comparison method evaluated differences between positions and bones of the location of the rotation axis. The mean and 95% confidence interval described rotation of the scaphoid and lunate. To test our hypothesis that the capitate and third metacarpal behave as a single rigid body, paired Student's *t*-test compared the magnitudes of flexion-extension rotation. We evaluated deviations of contact area from neutral grip using a 1-way repeated measures analysis of variance followed by a Holm-Sidak pairwise comparison procedure. Finally, we determined whether the contact center was beyond 1 mm of its location in neutral grip independently, for each articulation, by performing a 1-sample *t*-test with a hypothetical mean of 1 mm.

RESULTS

The wrist was extended 24° ± 13° in neutral grip, flexed 92° ± 8° in extreme flexion, and extended 78° ± 5° in extreme extension (Fig. 3). The wrist was ulnar deviated in neutral grip, extreme flexion, and extreme extension (9° ± 6°, 9° ± 6°, and 11° ± 8°, respectively). The orientation of the rotation axes of the third metacarpal and capitate from neutral grip to extreme extension and extreme flexion was within 1% of the flexion-extension axis defined by the RCS (Fig. 4, Table 1). The scaphoid and lunate rotation axes were also oriented within 1% of the flexion-extension axis of the RCS when the wrist moved from neutral grip to extreme flexion. However, the scaphoid and lunate exhibited larger out-of-plane motions during extreme extension, with 4% and 8% deviations from the flexion-extension axis of the RCS, respectively. The variability in rotation axis orientation was small, ranging from 5° to 8° (Table 1).

The rotation axes of the scaphoid and lunate from neutral grip to extreme flexion and from neutral grip to extreme extension were located near the proximal articular surface of the capitate (Fig. 5). They were dorsal to the midpoint of the proximal pole of the capitate in extreme extension and volar to the midpoint in extreme flexion. There were no significant differences ($P = .46$) between the locations of the scaphoid and lunate rotation axes in extreme extension. However, in extreme flexion, the lunate rotation axis was located an average of 1.4 mm more proximal and an average of 4.6 mm more volar than the scaphoid rotation axis ($P < .001$). The third metacarpal rotation axis

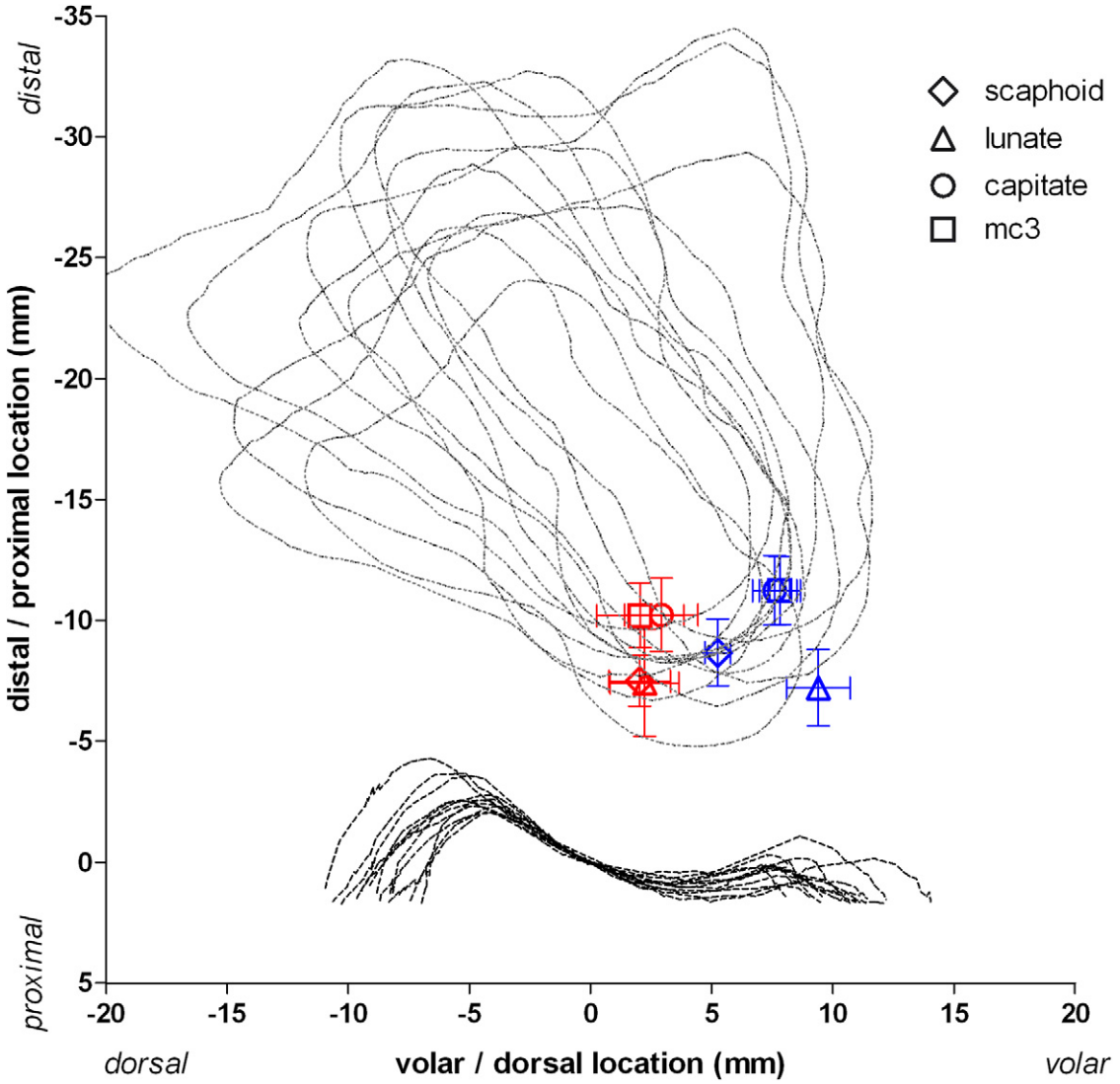

FIGURE 5: Helical rotation axis intersection in the sagittal plane plotted with sagittal outlines of each subject's radius and capitate in neutral grip. Red points indicate the location of the rotation axis when the wrist moves from neutral grip to extreme extension, and blue points indicate the location of the rotation axis when the wrist moves from neutral grip to extreme flexion.

was located an average of 0.9 mm more dorsal ($P < .050$) than the capitate in extreme extension.

In extreme flexion, the scaphoid flexed 70% (confidence interval [CI, 66% to 73%) and the lunate flexed 46% (CI, 43% to 49%) of capitate flexion (Fig. 6). In extreme extension, the scaphoid extended 74% (CI, 67% to 82%) and the lunate extended 42% (CI, 33% to 50%) of capitate extension. The third metacarpal flexed 1.0° ± 1° ($P < .050$) farther than the capitate in extreme flexion and extended 4° ± 2° ($P < .001$) farther than the capitate in extreme extension (Table 2).

From neutral grip to extreme flexion, the radius-scaphoid contact center shifted 5.5 ± 1.0 mm toward the radial styloid and volar ridge of the radius, whereas in extreme extension it shifted dorsally 2.4 ± 1.0 mm (Fig. 7). At extreme flexion, the contact areas of the lunate and scaphoid on the radius decreased 39% ± 22% and 66% ± 13% ($P < .050$), respectively, from their values at neutral grip (Table 3). In extreme extension, the contact area of the lunate and scaphoid increased ($P < .050$) 45% ± 22% and 13% ± 16%, respectively, from their values at neutral grip.

The capitate-scaphoid contact center was consistently located on the radial aspect of the proximal pole of the capitate. The scaphoid-capitate contact center shifted 3.3 ± 1.0 mm ($P < .050$) toward the distal

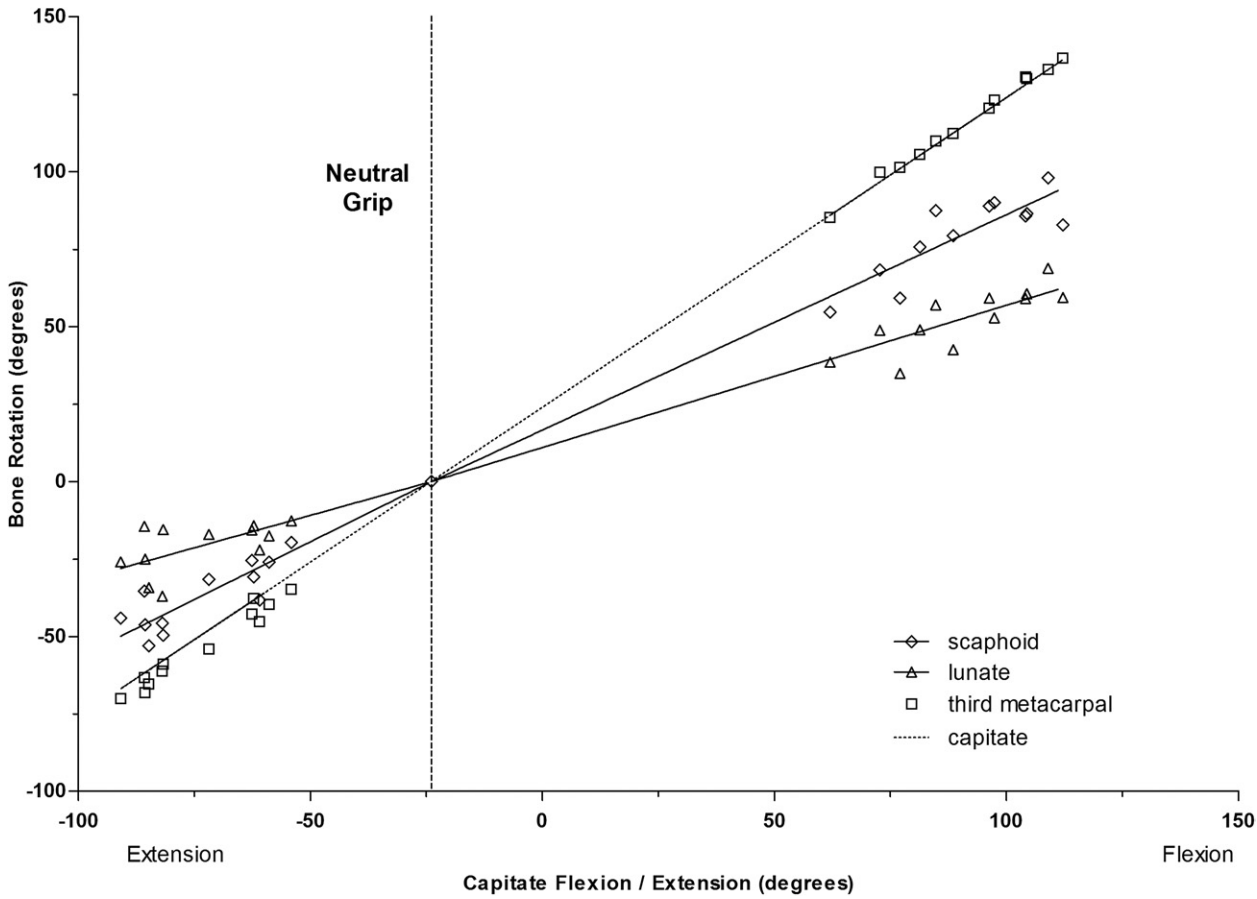

FIGURE 6: Scaphoid, lunate, third metacarpal, and capitate flexion-extension rotation versus capitate rotation from neutral grip to extreme flexion and extreme extension. The dotted line represents capitate flexion-extension versus capitate flexion-extension. During extension, data points below the dotted line indicate that the bone is extending less than the capitate. During flexion, data points above the dotted line indicate that the bone is flexing less than the capitate. The scaphoid and lunate rotated less than the capitate in both extreme flexion and extreme extension, whereas the third metacarpal rotated slightly farther than the capitate during extreme flexion and extreme extension.

tubercle of the scaphoid when the wrist was in extreme flexion. The contact centers of the capitate and lunate were located centrally in neutral grip, volarly in extreme flexion, and dorsally in extreme extension ($P < .050$). The contact area consistently increased ($P < .050$) from extreme flexion to extreme extension at each articulation of the midcarpal joint (Table 3).

DISCUSSION

This study describes the kinematics of the scaphoid, lunate, capitate, and third metacarpal at extreme wrist flexion and extension. When the wrist is loaded at extremes, wrist position is defined by the position of the forearm and an externally applied load. Several *in vivo* studies have evaluated 3-dimensional wrist postures throughout the range of active motion (approximately 60° flexion to 60° extension) using markerless tracking techniques similar or identical to those used in the present study.[2,13,14] These studies of active wrist motion have shown that from neutral to wrist extension, the scaphoid and capitate extend nearly as a single rigid body (range, 86% to 99%), whereas the lunate extends an average of 64% (range, 63% to 68%) of the amount the capitate extends.[2,13,14] During extreme loaded wrist extension, however, the scaphoid and lunate extend only 74% (CI, 67% to 82%) and 42% (CI, 33% to 50%) as much as the capitate. We note that the confidence intervals fall outside the range of values reported in the literature. Therefore, the scaphoid and lunate rotate less compared with the capitate during extreme extension but rotate with the capitate in active extension. In active extension, the capitate rotates less than it does in loaded extreme extension (approximately 60° compared with 78°). For scaphoid and lunate rotation to be less than the capitate, as seen in active wrist range of motion, their motion must be restricted along the path. We postulate that

TABLE 2. Average (1 SD) Rotation About and Translation Along the Helical Axis From the Neutral Grip Position*

		X		Y		Z	
Bone	Motion	Rotation (°)	Translation (mm)	Rotation (°)	Translation (mm)	Rotation (°)	Translation (mm)
Third metacarpal	Extension	0.05 (4.0)	0.04 (0.07)	–53.4 (12.7)	0.31 (0.86)	4.5 (8.6)	–0.15 (0.30)
	Flexion	4.7 (8.3)	0.07 (0.07)	115.7 (15.9)	1.2 (1.0)	−2.6 (10.1)	−0.01 (0.11)
Capitate	Extension	−0.13 (3.5)	0.02 (0.07)	−49.5 (13.0)	0.61 (0.67)	5.7 (7.8)	−0.17 (0.27)
	Flexion	3.9 (7.4)	0.05 (0.08)	114.7 (15.7)	1.2 (0.9)	−3.1 (10.4)	−0.01 (0.13)
Scaphoid	Extension	−5.1 (2.5)	0.17 (0.08)	−37.1 (10.7)	1.2 (0.4)	10.1 (4.5)	−0.36 (0.20)
	Flexion	1.0 (5.5)	0.01 (0.08)	79.8 (13.0)	0.79 (0.67)	−1.5 (7.1)	−0.02 (0.08)
Lunate	Extension	−1.6 (1.7)	0.07 (0.09)	−21.0 (8.1)	1.2 (0.4)	8.5 (3.7)	−0.51 (0.25)
	Flexion	0.14 (4.8)	−0.01 (0.2)	52.6 (10.1)	1.9 (0.7)	8.9 (5.2)	0.36 (0.25)

*X, Y, and Z correspond to the pronation-supination, flexion-extension axis, and ulnar-radial deviation components, respectively.

this restriction occurs between the end range of active motion (when the rotation of the scaphoid and lunate is closer to that of the capitate) and extreme extension when the volar ligaments are maximally strained and the scaphoid impinges on the dorsal ridge of the scaphoid facet. A likely result of this mechanical impingement is unbalanced compensatory forces of the scaphoid by its supporting ligaments. Scaphoid waist fractures or ruptures of the scapholunate ligament may result when these unbalanced forces exceed each structure's ability to withstand them. Although the motion between the third metacarpal and the capitate at extreme extension was small, this may be the etiology of carpal boss formation, because it has been suggested that repetitive excessive motion at this joint can lead to spur formation.[25]

In contrast, the contribution of scaphoid and lunate flexion to capitate flexion during extreme flexion was similar to previous *in vivo* reports of active flexion.[2,13,14] When combined, these studies report a range of 63% to 73% and 31% to 46% for the scaphoid and lunate, respectively.[2,13,14] We found that the scaphoid flexed 70% (CI, 66% to 73%) and the lunate flexed 46% (CI, 43% to 49%) of capitate flexion. These findings are not surprising given that the dorsal ligamentous restraints are considered to be thin and weak compared with the volar ligaments.[26] Therefore, these ligaments may allow a greater range of motion during wrist flexion before restraining the scaphoid and lunate. Because the volunteers flexed until they felt discomfort, we cannot safely determine whether the wrist is capable of achieving further extreme flexion with subsequent scaphoid and lunate restriction. The third metacarpal flexed only 1° farther than the capitate during extreme flexion. This difference is on the order of our measurement error and is unlikely to be clinically significant.

We quantified joint space characteristics with subchondral bone surface measurements, which do not represent physical contact between adjacent bones. We used joint space measurements as a surrogate for contact measurements because CT is unable to resolve articular cartilage in the intact joint. They are useful in elucidating which areas on 2 opposing surfaces move closer to one another without the need for cartilage contact estimation. In extreme flexion, the joint contact center of the scaphoid on the radius moved radial and distal, approaching the radial styloid and the volar ridge of the radius. In addition, the contact area decreased 66% from neutral grip, which suggests less congruence between the articulating surfaces. We postulate that the lunate follows a smooth rotation (likely because of its highly congruent and nearly hemispherical contour), whereas the scaphoid cantilevers on the volar radial lip.

The rotation axis of the capitate was more proximal in extreme positions compared with its position in the proximal pole during active wrist motion.[15,27,28] These findings indicate that in extreme flexion and extension, the capitate begins to rock within the lunate fossa rather than rotating within because of volar and dorsal impingement of the capitate on the lunate during extreme flexion and extreme extension.

The primary limitation of this study is the inference of motion from 3 static positions. The helical axis assumes that the motions between the neutral grip position and those at the end range of flexion-extension are at constant rate and in a single direction. Although we can infer the general behavior of the carpals as they move from neutral

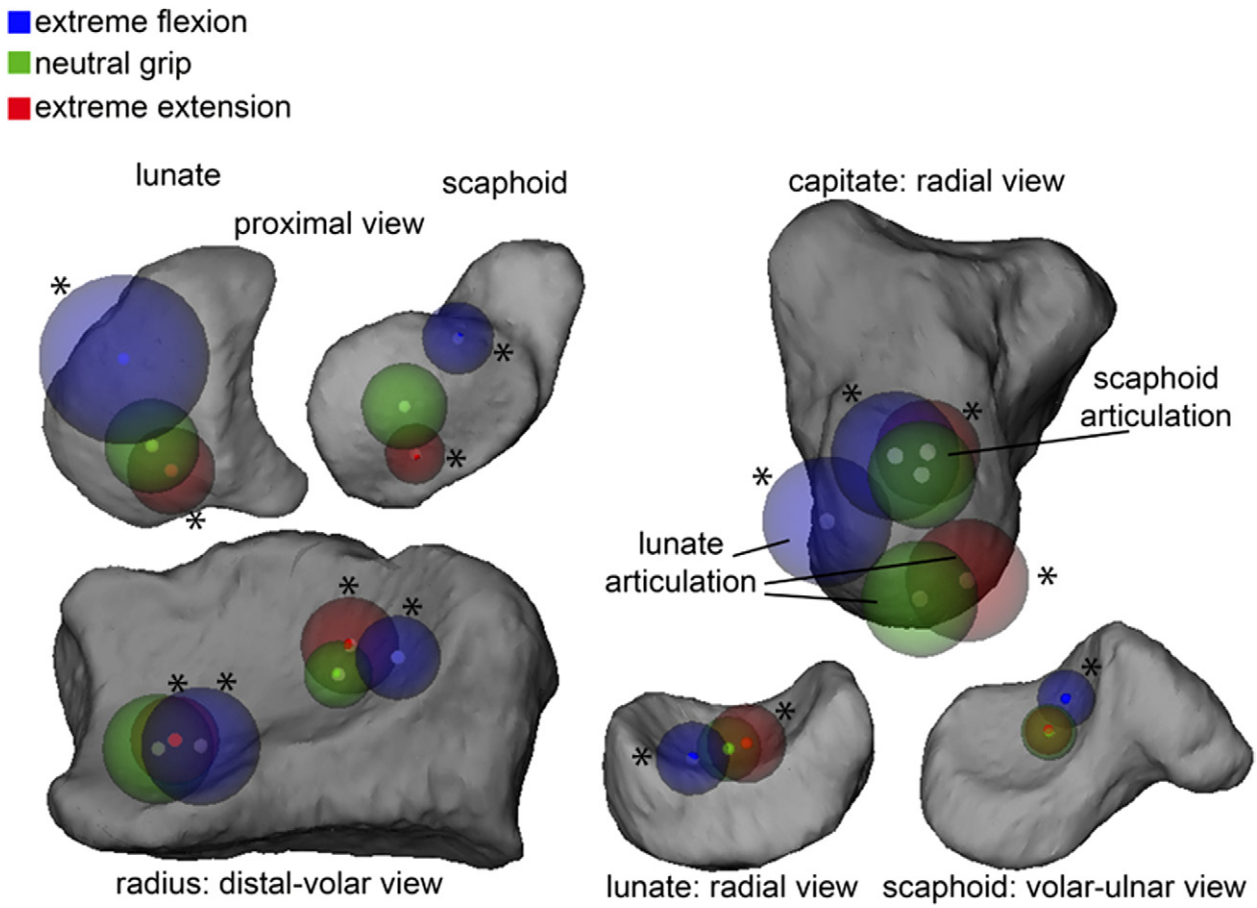

FIGURE 7: The mean (small central sphere) and standard deviation (large sphere) of the location of the joint contact center in all 3 wrist positions. Asterisk denotes a significant difference ($P < .050$) in the contact center location compared with neutral grip. At the radiocarpal joint (left), as the wrist moved from extreme extension to extreme flexion, the contact area decreased. Note the shift of the radius-scaphoid contact center toward the radial styloid in extreme flexion. At the midcarpal joint (right), the capitate exhibited a rocking motion on the lunate as it moved from neutral grip to extreme flexion or extreme extension. Also note the consistency in the capitate-scaphoid contact center location in all 3 positions. However, the contact center shifted toward the distal tubercle of the scaphoid in extreme flexion.

TABLE 3. Percent Increase or Decrease of Contact Area From Neutral Grip at the Radiocarpal and Midcarpal Joints, and Distance of Contact Center From Neutral Grip*

		% Change in Contact Area		Change in Contact Center (mm)	
Joint	Bone	Neutral Grip to Flexion	Neutral Grip to Extension	Neutral Grip to Flexion	Neutral Grip to Extension
Radiolunate	Radius	−40.0 (22.0)*	45.3 (21.6)*	3.9 (1.8)*	1.8 (0.7)*
	Lunate	−45.2 (19.0)*	46.6 (26.2)*	7.0 (3.0)*	2.5 (1.3)*
Radioscaphoid	Radius	−65.5 (12.6)*	13.2 (16.1)*	5.5 (1.0)*	2.4 (1.0)*
	Scaphoid	−62.4 (14.6)*	23.3 (26.1)*	8.0 (1.8)*	5.2 (1.2)*
Lunocapitate	Lunate	−9.1 (10.4)	7.2 (6.2)	3.0 (1.4)*	1.5 (0.5)*
	Capitate	−1.7 (13.8)	13.6 (10.1)*	7.7 (1.2)*	3.3 (1.2)*
Scaphocapitate	Scaphoid	−22.9 (0.5)*	9.4 (4.3)*	3.3 (1.0)*	0.8 (0.5)
	Capitate	−23.4 (10.3)*	15.3 (6.7)*	2.4 (0.6)*	1.5 (0.6)*

Data represent mean (± SD).
*Statistical significance ($P < .050$) from neutral grip.

to extreme flexion and extension, we cannot address nuances in kinematic patterns during intermediate positions. This study aimed to determine wrist kinematics in extreme loaded positions. Whereas targeting 98 N in extreme extension and requiring loading to resistance in extreme flexion was sufficient to load the wrist, we cannot address differences in wrist kinematics as a function of load. We did not measure active wrist positions in the current study because the patients pushed the palm of the hands against the weight scale. Therefore, we cannot perform a direct statistical comparison between loaded extreme and active motion. We did not constrain wrist position in the radial-ulnar plane during experimentation, nor did we measure extreme radial and ulnar deviation. Our analysis reports that subjects preferred to position the wrists in approximately 10° ulnar deviation during all 3 wrist positions of this study. We postulate this may have been because subjects attempted to keep the wrist in a more stable position during testing[29] and because of the forearm posture required for central hand placement on the scale at the extremes of motion.

This study of the intact wrist demonstrates that the motion of the carpus when the wrist is loaded in extension shifts toward the midcarpal joint, and gives insight into the vulnerability of the scaphoid and scapholunate interosseous ligament to injury in extreme wrist extension. Future studies of extreme wrist positions, when the carpal ligaments are engaged, may provide new insights into ligament function and allow clinicians to optimize treatment strategies.

REFERENCES

1. Crisco JJ, Coburn JC, Moore DC, Akelman E, Weiss AP, Wolfe SW. In vivo radiocarpal kinematics and the dart thrower's motion. *J Bone Joint Surg Am.* 2005;87(12):2729–2740.
2. Goto A, Moritomo H, Murase T, Oka K, Sugamoto K, Arimura T, et al. In vivo three-dimensional wrist motion analysis using magnetic resonance imaging and volume-based registration. *J Orthop Res.* 2005;23(4):750–756.
3. Moritomo H, Murase T, Goto A, Oka K, Sugamoto K, Yoshikawa H. In vivo three-dimensional kinematics of the midcarpal joint of the wrist. *J Bone Joint Surg Am.* 2006;88(3):611–621.
4. Savelberg HH, Kooloos JG, de Lange A, Huiskes R, Kauer JM. Human carpal ligament recruitment and three-dimensional carpal motion. *J Orthop Res.* 1991;9(5):693–704.
5. Werner FW, Short WH, Fortino MD, Palmer AK. The relative contribution of selected carpal bones to global wrist motion during simulated planar and out-of-plane wrist motion. *J Hand Surg Am.* 1997;22(4):708–713.
6. Majima M, Horii E, Matsuki H, Hirata H, Genda E. Load transmission through the wrist in the extended position. *J Hand Surg Am.* 2008;33(2):182–188.
7. Lee SK, Park J, Baskies M, Forman R, Yildirim G, Walker P. Differential strain of the axially loaded scapholunate interosseus ligament. *J Hand Surg Am.* 2010;35(2):245–251.
8. Webb BG, Rettig LA. Gymnastic wrist injuries. *Curr Sports Med Rep.* 2008;7(5):289–295.
9. Mayfield JK. Mechanism of carpal injuries. *Clin Orthop Relat Res.* 1980;(149):45–54.
10. An KN, Korinek SL, Kilpela T, Edis S. Kinematic and kinetic analysis of push-up exercise. *Biomed Sci Instrum.* 1990;(26):53–57.
11. Ishikawa J, Cooney WP III, Niebur G, An KN, Minami A, Kaneda K. The effects of wrist distraction on carpal kinematics. *J Hand Surg Am.* 1999;24(1):113–120.
12. Kobayashi M, Berger RA, Linscheid RL, An KN. Intercarpal kinematics during wrist motion. *Hand Clin.* 1997;13(1):143–149.
13. Moojen TM, Snel JG, Ritt MJ, Kauer JM, Venema HW, Bos KE. Three-dimensional carpal kinematics in vivo. *Clin Biomech.* 2002; 17(7):506–514.
14. Wolfe SW, Neu C, Crisco JJ. In vivo scaphoid, lunate, and capitate kinematics in flexion and in extension. *J Hand Surg Am.* 2000;25(5):860–869.
15. Neu CP, Crisco JJ, Wolfe SW. In vivo kinematic behavior of the radio-capitate joint during wrist flexion-extension and radio-ulnar deviation. *J Biomech.* 2001;34(11):1429–1438.
16. Patterson RM, Nicodemus CL, Viegas SF, Elder KW, Rosenblatt J. High-speed, three-dimensional kinematic analysis of the normal wrist. *J Hand Surg Am.* 1998;23(3):446–453.
17. Kazuki K, Kusunoki M, Shimazu A. Pressure distribution in the radiocarpal joint measured with a densitometer designed for pressure-sensitive film. *J Hand Surg Am.* 1991;16(3):401–408.
18. Kobayashi M, Garcia-Elias M, Nagy L, Ritt MJ, An KN, Cooney WP, et al. Axial loading induces rotation of the proximal carpal row bones around unique screw-displacement axes. *J Biomech.* 1997; 30(11-12):1165–1167.
19. Hara T, Horii E, An KN, Cooney WP, Linscheid RL, Chao EY. Force distribution across wrist joint: application of pressure-sensitive conductive rubber. *J Hand Surg Am.* 1992;17(2):339–347.
20. Crisco JJ, McGovern RD, Wolfe SW. Noninvasive technique for measuring in vivo three-dimensional carpal bone kinematics. *J Orthop Res.* 1999;17(1):96–100.
21. Marai GE, Laidlaw DH, Crisco JJ. Super-resolution registration using tissue-classified distance fields. *IEEE Trans Med Imaging.* 2006;25(2):1–11.
22. Coburn JC, Upal MA, Crisco JJ. Coordinate systems for the carpal bones of the wrist. *J Biomech.* 2007;40(1):203–209.
23. Kobayashi M, Berger RA, Nagy L, Linscheid RL, Uchiyama S, Ritt M, et al. Normal kinematics of carpal bones: a three-dimensional analysis of carpal bone motion relative to the radius. *J Biomech.* 1997;30(8):787–793.
24. Marai GE, Crisco JJ, Laidlaw DH. A kinematics-based method for generating cartilage maps and deformations in the multi-articulating wrist joint from CT images. *Conf Proc IEEE Eng Med Biol Soc.* 2006;(1):2079–2082.
25. Artz TD, Posch JL. The carpometacarpal boss. *J Bone Joint Surg Am.* 1973;55(4):747–752.
26. Taleisnik J. The ligaments of the wrist. *J Hand Surg Am.* 1976;1(2):110–118.
27. Rainbow MJ, Crisco JJ, Moore DC, Wolfe SW. Gender differences in capitate kinematics are eliminated after accounting for variation in carpal size. *J Biomech Eng.* 2008;130(4):041003.
28. Youm Y, Flatt AE. Kinematics of the wrist. *Clin Orthop.* 1980; (149):21–32.
29. O'Driscoll SW, Horii E, Ness R, Cahalan TD, Richards RR, An KN. The relationship between wrist position, grasp size, and grip strength. *J Hand Surg Am.* 1992;17(1):169–177.